

Antenna Spacing in MIMO Indoor Channels

V. Pohl, V. Jungnickel, T. Haustein, C. von Helmolt
Heinrich-Hertz-Institut für Nachrichtentechnik Berlin GmbH
Einsteinufer 37, 10587 Berlin, Germany,
e-mail: pohl@hhi.de

Abstract – We study the relation between antenna spacing and capacity of MIMO channels for indoor environments using a ray tracing program. It has been confirmed also by measurements that in rich scattering environments an antenna spacing below 0.5λ is sufficient to reach nearly the full capacity predicted for multiple-antenna arrays in ideal and uncorrelated Rayleigh fading channels.

1. INTRODUCTION

Multiple-element antenna arrays (MEAs) at both the transmitter (Tx) and the receiver (Rx) offer an enormous increase in capacity compared to systems with single antennas. Huge capacity was predicted by assuming independent Rayleigh fading between pairs of antennas [1]. The channel capacity may be significantly smaller when the fading is correlated [2]. In an indoor scenario where both the Tx and the Rx are in the same room, multiple reflections at the walls guarantee a rich scattering environment and the fades between the antennas will be uncorrelated as long as the antenna spacing is sufficiently large. The question is, how small the antenna array can be made without losing a significant amount of capacity? There are widely varying results found in the literature. In [3], based on ray tracing simulations, it was found that increasing the antenna spacing at both the Tx and the Rx to 3λ will help to achieve higher capacity. In [4] and [5], on the other hand, it was found, that in environments with spatial uniformly distributed scatterers no significant increase in the capacity is observed if the inter-element spacing is increased above $\lambda/2$.

In order to investigate the influence of the inter-element spacing on the capacity in more detail, measurements have been performed which have been compared with simulations obtained from a simple ray tracing tool.

This paper is organised as follows: Section II gives a detailed description of the simulation tool. In Section III the influence of the inter-element spacing in a MEA onto the capacity of a MIMO system is investigated. Section IV gives a short summary.

II. THE SIMULATION TOOL

Indoor environments are characterised by an immense number of possible paths between the Tx and Rx due to multiple reflections at the walls. At the Rx all these incoming rays are added according to their different amplitude, phase, polarisation, arrival time and form so the overall channel response. The differences in all the incoming rays and the enormous number of them may help to decorrelate the different antenna signals even if the power of these single

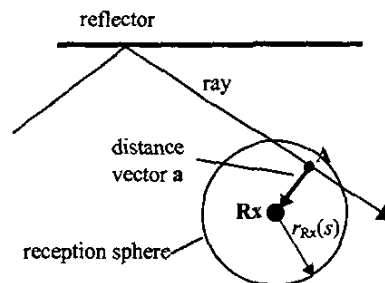


Fig.1: Reception sphere at the Rx

rays is small. Therefore it seems desirable to have no limit in the number of reflections in the model, at least in principle.

Presently, our simulation program describes propagation inside an empty room with dielectric walls. The propagation of the electromagnetic field is modeled as the propagation of linearly polarised plane waves on discrete paths. In a first step, a list of these paths between the Tx and the Rx is created using a monte carlo method similar to the algorithm which was used by the authors for modelling the infrared indoor channel [6]. The propagation of light is best described by photons i.e. by the energy flow. But the detection principle is different for light- and radio waves. Therefore the simulation tool has been modified to allow the calculation of the electric field. Based on the path list impulse response and transfer function are easily determined by calculating the electrical field for each path at the Rx site.

A. Path search

Starting at the Tx, a ray with random polarisation is send into a random direction. If the ray hits a wall, the reflection factor of the electrical field ρ (i.e. the ratio of the electrical field of the incoming- and reflected ray $\rho = |\mathbf{E}_{\text{refl}}|/|\mathbf{E}_{\text{in}}|$) is determined using Fresnel's formula, taking into account the polarisation and angle of incidence of the ray. Then a random number, uniformly distributed on $[0,1]$, is created. If this number is greater than ρ the tracing of this ray is stopped (i.e. the ray is absorbed by the wall) and the same procedure is started at the Tx with a new ray. Otherwise the direction of the reflected ray is determined and the path of this ray is traced further.

After each reflection it is tested whether the ray hits the Rx or not. To this end the shortest distance $a=|a|$ (see Fig. 1) between the ray path and the Rx position is determined. If a is smaller then the radius of the reception sphere around the

Rx, the ray is received. Otherwise ray tracing is continued with the same ray.

The radius $r_{Rx}(s)$ of the reception sphere depends on the total path length s from the Tx up to the point A, which marks the closest distance between the ray and the Rx. To explain this we consider the line-of-sight (LOS) path between the Tx and the Rx. The Tx sends rays omni-directionally into the room. If the radius of the reception sphere would be constant ($r_{Rx}=r_0$) then the number of received paths at the Rx would be proportional to $r_{Rx}^2/s^2=r_0^2/s^2$ i.e. proportional to the received power. But the receiving antenna detects the electrical field, and all the different paths arriving at the Rx are summed up according to their field components. Since the electrical field components of a dipole, for instance, are attenuated reciprocally to the distance s ($\sim 1/s$) from the source, we make the radius of the reception sphere proportional to the square root of the path length: $r_{Rx}(s) \sim \sqrt{s}$. Then the number of the received paths will be proportional to $r_{Rx}^2(s)/s^2=1/s$ i.e. proportional to the field strength. In other words, the probability that a ray emitted by the Tx will hit the Rx (i.e. the probability that this single path between the Tx and Rx is found) is proportional to $1/s$ i.e. proportional to the field strength which this ray will produce at the Rx position. This model ensures that the probability for a path between Tx and Rx to be found is proportional to the contribution which this ray will have on the whole received signal. So this algorithm will find the most important (strongest) paths at first. Note, that there is actually no restriction in the number of reflections a ray can undergo. If the radius of the reception sphere would be held constant, long paths would be discriminated. If, on the other hand, the radius of the reception sphere would be made proportional to s (as proposed in [7]) long paths would be preferred. In [7] this linearly growth of the radius was introduced to ensure that no ray path is counted twice. This problem is solved here in a different way: If every reflector in the room gets a unique number then a possible path between the Tx and the Rx is uniquely determined by the sequence of the numbers of the reflectors this ray passes. In our simple environment there are just six walls (1,...,6) and so there exists, for instance, exactly one ray who is first reflected at wall 2, then at wall 3, then at wall 6 and then hits the receiver. Therefore this path is characterised uniquely by the sequence {2,3,6}. By comparing these sequences, it is easy to detect if a path was found twice by the search algorithm.

During the acquisition of paths, the reflectivity of the walls is set much higher than in reality to ensure that all important paths are included. If non new path is found out of 10^6 successively emitted test rays, the search algorithm is stopped. We have always used at least 10^4 different paths between the Rx and Tx. To find these 10^4 paths, the algorithm, written in C++, needs typically a couple of hours on a customary 2 GHz PC. At the end of this initial search algorithm we have a list of possible paths. To each path the unique sequence of reflectors and the start direction r_i of the ray is stored.

B. Correction of the paths

During the search algorithm the Rx is not a single point but a sphere centred at the Rx position. Therefore, the paths will

not end exactly at the Rx position. But these differences can easily be corrected for every single path: Let r_i be the normalised vector ($|r_i|=1$) pointing into the start direction of the i^{th} path. At first a orthogonal ray-coordinate system at the Tx is constructed with the axes ξ and ζ perpendicular to the ray path i.e. perpendicular to r_i . A copy of this coordinate system (ξ' and ζ') is then carried along the ray path. At every reflection point these axes ξ' and ζ' are reflected according to the usual reflection laws (i.e. the components of these axes in the plane of incidence are flipped vertically whereas the perpendicular components remain in the same direction). At the end point A of the ray path (see Fig. 1) the distance vector a is determined. It describes how far and in which direction the Rx was missed, and it is determined by means of the ray-coordinate system: $a=\alpha_1\xi'+\alpha_2\zeta'$. The start direction of the ray can now be corrected by $r_i=r_i-\Delta r$ with the correction vector $\Delta r=(\alpha_1\xi'+\alpha_2\zeta')/s$, where s is again the total path length. Doing this correction for every single path, we end up with a path list, in which all paths start at the Tx position and end at the Rx position, exactly.

C. Transfer function

Based on the path list the impulse response $h(t)$ can be obtained by calculating the attenuation of the electrical field along each path taking into account the antenna characteristic and polarisation, reflections at the walls and free space attenuation reciprocally with the path length: Starting at the Tx with the assumption that the antenna is driven by a harmonic current of frequency f and with amplitude $I_0=1$: $I_{Tx}(t)=I_0\cos(2\pi f t)$ and knowing the antenna characteristic we can determine the components of the electromagnetic field in the direction of every path. Following the path, the attenuation of the field components are determined, and from the knowledge of the Rx antenna characteristic and the direction of arrival of the rays at the Rx, the induced current amplitude I_k in the Rx antenna is determined for every single ray. From the path length of each ray the delay time τ_k is

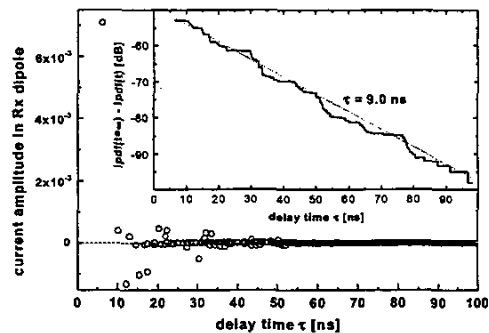


Fig. 2: Example of an impulse response in a room (5x4x3 m) with dielectric walls ($\epsilon_r=4.0$). The inset shows that the received power decays exponentially in time

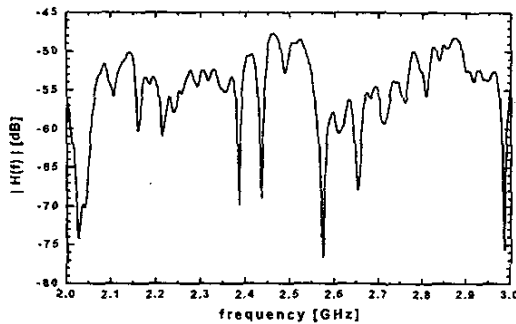


Fig. 3: Transfer function corresponding to the impulse response in Fig. 2.

determined. So the impulse response is written as

$$h(t) = \sum_k I_k \delta(t - \tau_k). \quad (1)$$

Note that I_k depends in general on the frequency f (if for example $\lambda/2$ -dipoles are used at Tx and Rx the I_k 's are proportional to $1/f$) and since we take into account the polarisation, I_k can be positive or negative. Fig. 2 shows an example of such an impulse response. Every point corresponds to a single path with the induced current amplitude I_k on the vertical axis and the delay time τ_k on the horizontal axis. The integral power delay function $\text{ipdf}(t)$

$$\text{ipdf}(t) := \int_0^t |h(s)|^2 ds \quad (2)$$

in the inset indicates an exponential decay of signal power in the room. Fig. 3 shows a part of the wide-band transfer function $H(f)$ calculated by Fourier transform of the impulse response:

$$H(f) = \sum_k I_k e^{-2\pi f \tau_k} \quad (3)$$

Once the path list is known, all other parameters (antenna characteristics, reflectivity of the walls) can be changed easily to calculate the transfer function again with these new parameters.

D. Antenna arrays

To calculate the transfer function between the same Tx but a neighbouring Rx, the Rx is moved a small distance from the old position. Then the situation for all the rays is the same as shown in Fig 1, all rays will miss the exact Rx position a little. The only thing we need to do is to correct the path list as explained in subsection B. This correction of the paths takes only a few seconds compared to a couple of hours for a complete new path search. So we get the path list for the new antenna configuration very fast. If the distance between the old and the new Rx position is larger, the whole way should be divided into smaller segments and the paths should be

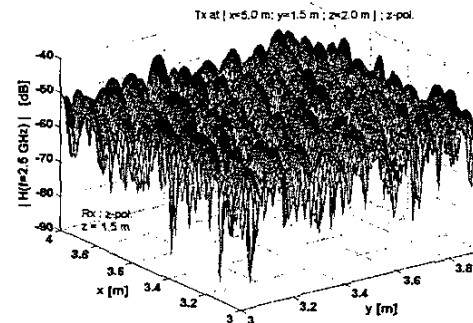


Fig. 4: Spatial variation of the (NLOS) signal amplitude over a square metre within a room ($7 \times 4 \times 3 \text{ m}^3$) with dielectric walls ($\epsilon_r=4.0$) and $f=2.5$ GHz

tracked from point to point. Based on this updated path list impulse response and transfer function can be calculated again. Fig. 4 shows the power profile, which is obtained with this method by moving the Rx in a regular grid. Of course the same method can be used to move the Tx to a different position, and so the transfer matrix of a channel with MEA at the Tx and at the Rx is easily determined. Since the paths connecting the Tx and Rx antennas remain essentially the same, this method seems especially suited for the investigation of the correlation in MEA signals. In this way we focus on the effect of the small changes in the transfer function due to the small differences in the positions of the single antenna elements.

III. ANTENNA SPACING

Now we want to use this ray tracing tool to investigate the influence of inter-element antenna spacing in a MEA system onto the capacity. We consider two different antenna configurations: In the first one the antenna spacing is changed only at one side (at the Rx). In the second scenario we study the behaviour if the antenna spacing is reduced at both the Rx and the Tx. In both scenarios the antenna arrays are placed about 1.9 m apart from each other in an empty rectangular room ($7 \times 4 \times 3 \text{ m}^3$) with perfect dielectric walls. The average reflectivity of the room $\langle R \rangle$ is changed by varying the relative dielectric constant ϵ_r of the dielectric walls. We used $\epsilon_r=4$ which results in an average reflectivity of about $\langle R \rangle=0.16$, and $\epsilon_r=60$ which results in $\langle R \rangle=0.6$. The average reflectivity was determined by monitoring the reflection coefficients at every reflection point during the ray tracing and averaging. Alternatively $\langle R \rangle$ can be calculated from the Fresnel's formula by assuming that all incident angles and all polarisation are equally likely. Both results coincided with each other.

Measurements indicate that the reflectivity in the rooms of the HHI building is typically quite high due to ferroconcrete used in the construction of the building. Since complex dielectric constants are not incorporated in our simulation

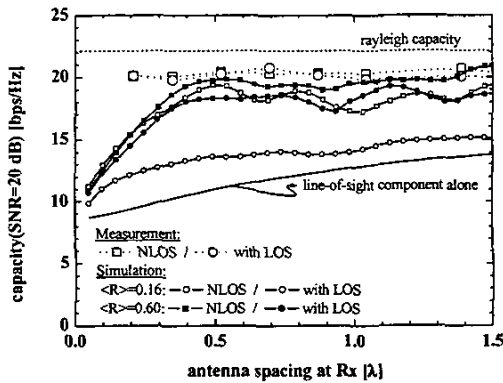


Fig. 5: Capacity with and without LOS component as function of the antenna spacing at the Rx. Simulation and measurement. The expected capacity for a perfect Rayleigh channel is shown for comparison

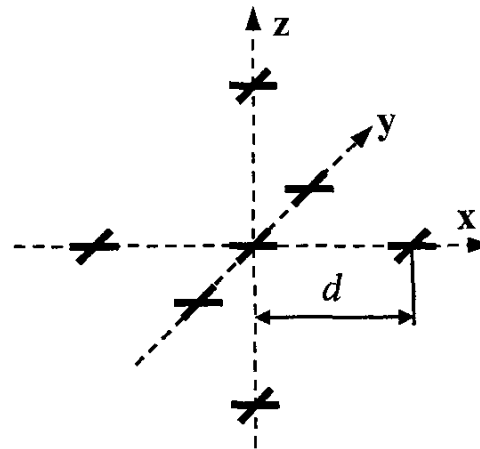


Fig. 6: Geometry of the antenna arrays: 7 antennas each with a x- and y-polarised dipole. Adjacent antennas are separated by $d=10$ cm.

tool up to now, we model this high reflectivity by large values for ϵ_r . We hope that this has only minor impact on our results since we are mainly focused on the antenna spacing in highly scattering environments, and it should be not significant which physical effect produces the scattering rays.

A. First Scenario

In this scenario the Tx consists of 4 dipole antennas placed at the corners of a rectangle with side length $l=14\text{cm}=2.45\lambda$ at the same height. Every dipole in this array has a different polarisation. The Rx is a linear array with 4 equally polarised dipoles and an inter-element antenna spacing of d . The ray-tracing program is used to calculate the transfer matrix H in dependence of the antenna spacing d . From the simulation we extracted also the matrix H_{LOS} corresponding to the line-of-sight (LOS) signal alone and the matrix H_{NLOS} which is the transfer matrix without the LOS component. Each matrix is normalised such that

$$\sum_{ij} |H_{ij}|^2 = 1 \quad (4)$$

where H_{ij} are the single complex entries in the matrices. From these matrices the capacity C was calculated using the formula stated in [1] for an average signal-to-noise ratio of $SNR=20$ dB at the receiver:

$$C(SNR) = \sum_{i=1}^n \log_2(1+SNR/n*\lambda_i^2) \quad (5)$$

where n is the number of transmit antennas ($n=4$ in our case) and λ_i are the singular values of the normalised transfer matrix H . Like in the measurement below, the average capacity was calculated from the results for 21 different frequencies between 5.1 and 5.3 GHz. For comparison, the capacity for a perfect Rayleigh channel is plotted. To this end 10^5 random matrices with independent, identically distributed

complex numbers (normal distribution with zero mean and variance $\sigma=1$) were generated and the average capacity was calculated.

Fig. 5 shows the results for two different values of the average reflectivity $\langle R \rangle$ in the room. Unlike the LOS component the capacity of the NLOS signal is nearly constant if the antenna spacing is greater than $d \approx 0.4\lambda$. If the reflectivity is high, the NLOS component dominates the behaviour of the overall channel, and so also the overall signal (with LOS) reaches nearly the full capacity already with an antenna spacing of around 0.4λ .

In the same figure measurement results are plotted as well. These measurements were done in the entrance hall of the institute building using the wideband vector channel sounder RUSK ATM [8]. The channel sounder operates at 5.2 GHz with a measurement bandwidth of 120 MHz. We calculated the average capacity from 20 different frequencies within the measurement bandwidth. The antenna arrays in the measurement were similar to the antennas used in the simulations. Tx and Rx were 10 m apart from each other. In the measurement results nearly no difference between the curves with and without LOS signal is observed, which indicates that the reflectivity of this room is quite high and so the LOS component has no impact on the result. Like in the simulation the measurement shows that an antenna spacing below 0.5λ is sufficient to get nearly the whole capacity of the rich scattering rayleigh channel. Surprisingly there is no decrease in the capacity below 0.5λ as expected from the simulation. The reason behind this is yet not fully understood. But these measurement results already confirm that the antenna spacing at the mobile terminal can indeed be made very small in indoor environments.

B. Second Scenario

We consider a Tx and Rx MEA as shown in Fig. 6. The ray-tracing program is used to calculate the wide-band

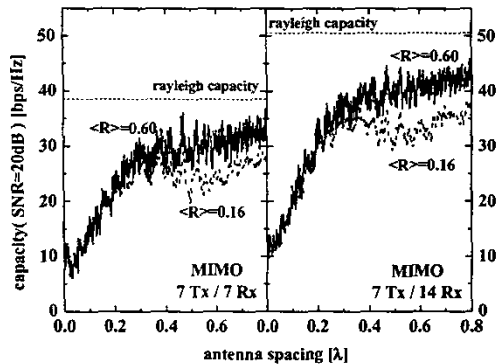


Fig. 7: Capacity vs. relative antenna spacing d/λ for to different antenna configurations of the NLOS component only.

transfer function from every Tx to every Rx antenna for frequencies from 0 up to 10 GHz. This results in the transfer matrix $H(f)$. Varying the frequency f we change also the effective antenna spacing d/λ . In Fig. 7 the capacity as a function of the relative antenna spacing d/λ is plotted for two different values of the average reflectivity $\langle R \rangle$ in the room. For the 7×7 configuration on the left side only the x-polarised dipoles of the MEAs are used, but for the 7×14 configuration on the right all 14 dipoles at the Rx are used. We see nearly the same behaviour as in scenario 1. Increasing the antenna spacing above $d=0.4\lambda$ results only in a small increase in capacity.

The results for both scenarios coincide with the measurement results reported in [5]. In all simulations and in the measurements we observed between 85% and 90% of the rayleigh capacity (i.e. the capacity which was predicted for completely uncorrelated antennas).

IV. SUMMARY

We have used ray-tracing to investigate the influence of the inter-element antenna spacing in multiple-element antenna array onto the capacity of the system. In this ray tracing simulation a large number of reflections is taken into account to get a realistic model of an indoor environment, which is characterised by multiple reflections at the walls. We found

that antenna spacing as small as 0.4λ may be sufficient to get about 90 % of the capacity which is possible by the use of multiple-element antenna arrays in ideal Rayleigh fading channels. Increasing the antenna spacing further will have no significant impact on the capacity. A measurement fully confirmed this result.

ACKNOWLEDGEMENT

The authors would like to thank our project partners MEDAV GmbH for the provision of the measurement equipment and the support during the measurement campaign.

REFERENCES

- [1] G.J. Foschini, „Layered space-time architecture for wireless communication in a fading environment when using multi-element antennas“, *Bell Labs Techn. J.*, 1,2 (Aut. 1996), pp. 41-59
- [2] D.-S. Shiu, G.J. Foschini, M.J. Gans, J.M. Kahn, „Fading correlation and its effect on the capacity of multi-element antenna systems“, presented at *ICUP98*, Florence, Italy, 1998
- [3] C.-N. Chuah, G.J. Foschini, R.A. Valenzuela, D. Chizhik, J. Ling, J.M. Kahn, „Capacity Growth of Multi-Element Arrays in Indoor and outdoor Wireless Channels“, *IEEE WCNC*, Chicago, Sept. 23.-28., 2000
- [4] A.G. Burr, „Channel capacity evaluation of multi-element antenna systems using a spatial channel model,“ in *Proc. of Millenium Conf. On Antennas & Propagation*, April 2000, Davos, Switzerland
- [5] M. Steinbauer, A.F. Molisch, A. Burr, R. Thomä, „MIMO channel capacity based on measurement results“, in *Proc. of the European Conf. on Wireless Technology*, Paris, Oct. 5.-6., 2000, pp. 52-55
- [6] V. Jungnickel, V. Pohl, S. Nönnig, C. von Helmolt, „A Physical Model of the Wireless Infrared Communication Channel,“ to appear in *IEEE JSAC, special issue on Channel and Propagation Models*, May 2002
- [7] K.-R. Schaubach, N.J. Davis, and T.S. Rappaport, „A ray tracing method for predicting path loss and delay spread in microcellular environments,“ in *Proc. of IEEE Veh. Technol. Conf.*, Denver, May 1992, pp. 932-935
- [8] R. Thomä, D. Hampicke, A. Richter, G. Sommerkorn, A. Schneider, U. Trautwein, and W. Wirnitzer, „Identification of time-variant directional mobile radio channels,“ *IEEE Trans. On Instrumentation and Measurement*, vol. 49, pp. 357-364, April 2000.